JTK: Jurnal Tadris Kimiya 11, 1 (June 2026): 37-57
Website: http://journal.uinsgd.ac.id/index.php/tadris-kimiya/index
ISSN 2527-9637 **(online) ISSN** 2527-6816 **(print)**

Microwave-Assisted Synthesis of Eggshell-Derived Hydroxyapatite for Antibacterial Toothpaste Enriched with Avocado Seed Powder and Extract

Gabrielle Callista Dwi Putri[1], Atiek Rostika Noviyanti[1*], Yudha Prawira Budiman[1] Suryana[2], and Azman Bin Ma'Amor[3]
[1]Department of Chemistry, Faculty of Mathematics and Natural Sciences Universitas Padjadjaran, Sumedang, 45363, Indonesia
[2]Department of Biology, Faculty of Mathematics and Natural Sciences, Universitas Padjadjaran, Sumedang 45363, Indonesia
[3]Department of Chemistry, University Malaya, Kuala Lumpur 50603, Malaysia
**E-mail: atiek.noviyanti@unpad.ac.id*

Received: May 2026; Accepted: June 2026; Published: June 2026

Abstract

Hydroxyapatite (HA) is a biomimetic material widely used in toothpaste due to its structural similarity to dental enamel. This study aimed to develop an antibacterial toothpaste using HA synthesized from eggshell waste via a microwave-assisted method and enriched with avocado seed (Persea americana Mill.). HA was prepared at a Ca/P ratio of 1.67 using EDTA as a chelating agent and characterized by XRD, FTIR, and SEM. The results confirmed the formation of HA with residual calcite and nanoscale morphology. The optimal EDTA:Ca ratio (0.5:1) yielded the highest HA fraction (82.5 wt%) and crystallinity (78.23%). All toothpaste formulations met physicochemical standards, with pH ranging from 8.93 to 10.0, foam stability between 72.4% and 94.1%, and spreadability between 3.0 and 4.7 cm. Antibacterial tests against Streptococcus mutans ATCC 25125 revealed that avocado seed powder exhibited strong initial inhibition (37.7 mm) but decreased after 30 days of storage, while the extract provided more stable activity (10.09 mm). These findings indicate the potential of combining HA with avocado seed derivatives as a natural and sustainable antibacterial toothpaste formulation. The finding that avocado seed extract exhibits more stable antibacterial activity than powder is particularly important for pharmaceutical industries and dental biomaterial development, as it highlights the necessity of using extract-based formulations to ensure long-term efficacy and shelf stability.

Keywords: antibacterial, avocado seed, hydroxyapatite, microwave-assisted, toothpaste

DOI: https://doi.org/10.15575/jtk.v11i1.55586

1. Introduction

Dental health is an essential component of overall human health, with dental caries remaining one of the most prevalent oral diseases worldwide. In Indonesia, the prevalence of dental caries reached 82.8% according to the 2023 National Health Survey, indicating that a large proportion of the population is still affected by this condition. Dental caries is a multifactorial disease caused by the interaction between cariogenic bacteria, salivary pH fluctuations, and fermentable carbohydrates, leading to the demineralization of enamel and dentin (Neel et al., 2016). The process is initiated by bacterial fermentation of dietary carbohydrates, producing acidic by-products

that lower oral pH and promote mineral loss. Microbiome dysbiosis further accelerates this process, involving acidogenic and acid-tolerant species such as *Streptococcus mutans, Lactobacillus spp., Scardovia wiggsiae,* and *Actinomyces spp* (Hasan et al., 2024). If untreated, early lesions such as white spot lesions may progress into deep cavities and eventually damage the dental pulp.

Although the global prevalence of dental caries has decreased by approximately 6% between 2018 and 2023, the severity remains high, particularly among children. National data indicate that the decay-missing-filled teeth (*dmft*) index in Indonesian children exceeds the World Health Organization (WHO) threshold for high severity, highlighting the urgent need for more effective preventive strategies (Hasan et al., 2024). Brushing teeth with fluoride-containing toothpaste twice daily is widely recognized as an effective preventive measure (Cocco et al., 2025). However, concerns have been raised regarding the excessive use of fluoride, particularly in children, which may lead to adverse effects such as enamel fluorosis. In addition, sodium lauryl sulfate (SLS), commonly used as a surfactant in toothpaste formulations, has been associated with oral mucosal irritation and ulcer formation (Daas et al., 2018). Although avocado seed has demonstrated promising antibacterial activity against oral pathogens, its incorporation into hydroxyapatite-based toothpaste presents several formulation challenges. Improper incorporation of avocado seed derivatives may lead to instability of bioactive compounds, microbial contamination during storage, phase separation, and reduced antibacterial efficacy, ultimately limiting the shelf life and effectiveness of the final product. Furthermore, no study has systematically compared the storage stability and antibacterial performance of avocado seed powder and avocado seed extract within a hydroxyapatite-based toothpaste matrix.

These concerns have driven the development of safer and more sustainable alternatives, particularly natural and biomimetic materials. Among these, hydroxyapatite (HA) has emerged as a promising candidate due to its high similarity to the mineral composition of enamel. HA is a biocompatible calcium phosphate material that promotes remineralization by supplying calcium and phosphate ions to demineralized regions and forming a protective apatite layer on the enamel surface (Anil et al., 2022; Imran et al., 2023). Moreover, HA can be synthesized from natural calcium sources such as eggshell waste, which contains approximately 98.43% calcium carbonate (Noviyanti, 2020), making it a sustainable and low-cost precursor.

Various synthesis methods have been developed to produce HA, including precipitation, sol–gel, hydrothermal, and microwave-assisted techniques (Baladi et al., 2023; Castro et al., 2022; Waardhani et al., 2025). Among these, microwave-assisted synthesis offers significant advantages, such as rapid heating, uniform energy distribution, shorter reaction time, and improved crystallinity (Perwiranegara et al., 2021; Stanislavov et al., 2018). This method enables efficient production of high-quality HA nanoparticles suitable for biomedical applications. Furthermore, the resulting HA nanoparticles exhibit high bioactivity and physicochemical properties that closely resemble the mineral phase of human hard tissues, making them particularly attractive for dental applications. In dentistry, HA has been widely investigated as a remineralizing agent due to its ability to promote mineral deposition, reduce enamel demineralization, and support the repair of early enamel lesions. These properties highlight the potential of HA for preventive and restorative oral health applications.

Despite its advantages, HA exhibits limited antibacterial activity, which restricts its effectiveness in inhibiting cariogenic bacteria such as *Streptococcus mutans* (Djayasinga et al., 2024). Therefore, the incorporation of natural antibacterial agents is necessary to enhance its functionality. Avocado seed (Persea americana Mill.) has been reported to possess strong antibacterial activity, with inhibition zones reaching 21.8 mm against S. mutans (Bujung et al., 2017). This activity is

attributed to the presence of bioactive compounds such as flavonoids, tannins, alkaloids, and saponins, which interfere with bacterial cell walls, membranes, and metabolic processes (Artaningsih et al., 2018; Beby et al., 2023). In addition, avocado seeds contain significant mineral content, including calcium (643.62 mg/100 g), which may contribute to enamel strengthening and remineralization (Fufa et al., 2025).

Avocado seeds can be utilized in both extract and powder forms. The extract form provides concentrated bioactive compounds with enhanced antibacterial activity, while the powder form retains natural mineral content that may support remineralization. According to Badan Pusat Statistik given the high production of avocados, reaching 919,508 tons in 2024, avocado seeds represent an abundant and underutilized natural resource. Previous studies have investigated HA-based toothpaste formulations and reported comparable remineralization performance to fluoride-containing toothpaste, although the results remain inconsistent (Irwansyah et al., 2022; Tschoppe et al., 2011). Despite these efforts, the exploration of HA from natural waste sources especially eggshell combined with novel plant-based antibacterial agents remains limited. However, studies combining HA derived from eggshell waste with natural antibacterial agents, particularly avocado seed in both extract and powder forms, remain limited.

This study aimed to develop an antibacterial toothpaste formulation using microwave-assisted hydroxyapatite (HA) synthesized from eggshell waste and enriched with avocado seed extract. The effects of different HA and avocado seed extract concentrations on the physicochemical properties and antibacterial activity against Streptococcus mutans were systematically evaluated to determine the optimal, sustainable, and effective formulation. In addition, previous studies on eggshell-derived hydroxyapatite have mainly focused on conventional precipitation, hydrothermal, or calcination-assisted methods. The application of a one-pot microwave-assisted synthesis route combined with optimization of the EDTA: Ca ratio for controlling phase composition and crystallinity remains largely unexplored. Therefore, this study provides a novel approach by integrating microwave-assisted hydroxyapatite synthesis with the comparative evaluation of avocado seed powder and extract in antibacterial toothpaste formulations.

2. Synthesis of Eggshell-Derived Hydroxyapatite

2.1. Materials

The materials used in this study were aquadest (H_2O), avocado seeds, chicken eggshells, CMC Na (Sigma Aldrich), diammonium hydrogen phosphate (DHP, Merck), avocado seed extract, 70% ethanol, ethylene diamine tetraacetic acid (EDTA, Merck), glycerol, sodium lauryl sulfate (SLS), menthol, sodium benzoate, and sodium saccharide.

2.2. Equipment

The equipment used included standard laboratory glassware, a 100-mesh sieve, a homogenizer, a centrifuge, filter paper, a condenser, a magnetic bar with a magnetic stirrer, a microwave oven (Samsung), a mortar and pestle, an oven, a pH meter (Ohaus), a planetary ball mill, a Fourier Transform Infrared Spectroscopy (FTIR) instrument, an X-Ray Fluorescence (XRF, EDAX) instrument, and an X-ray Diffraction (XRD, Bruker D8 Advance) instrument.

2.1.1. Preparation of Calcium Precursor

Eggshell waste was washed with distilled water, dried in an oven, and ground using a planetary ball mill. The powder was sieved to 100 mesh to obtain fine calcium carbonate ($CaCO_3$), which was subsequently characterized using X-ray fluorescence (XRF).

2.1.2. Microwave-Assisted Synthesis of Hydroxyapatite

Hydroxyapatite (HA) was synthesized following a modified method reported by Kumar & Girija (2013). $CaCO_3$ and diammonium hydrogen phosphate (DHP) were mixed at a Ca/P molar ratio of 1.67. EDTA was added as a chelating agent, followed by

the addition of distilled water to form a suspension. The mixture was stirred using a magnetic stirrer, and the pH was adjusted to 13 using NaOH. All aqueous solutions were prepared using carbonate-free distilled water to prevent interference from carbonate ions during the synthesis and washing processes.

The suspension was then subjected to microwave irradiation at 450 W and 2.45 GHz for 45 minutes (Sabu et al., 2019). These parameters were selected based on preliminary optimization trials, in which irradiation powers of 300, 450, and 600 W and durations of 30, 45, and 60 minutes were tested (Figure 1).

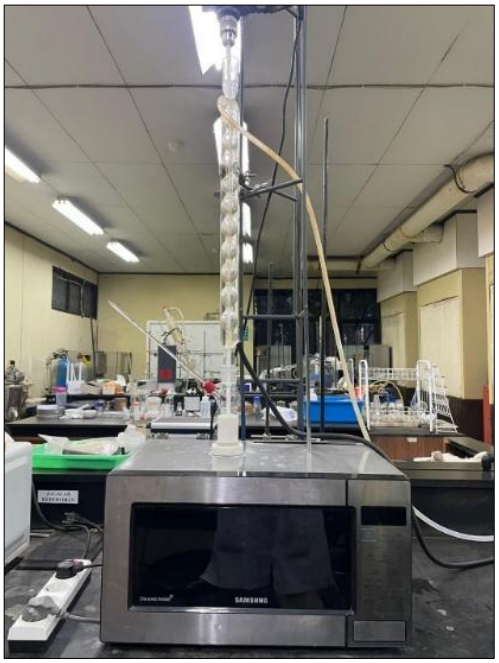

Figure 1. Microwave-assisted synthesis setup

The combination of 450 W and 45 minutes yielded the highest crystallinity and purity of the hydroxyapatite phase as confirmed by XRD analysis, while longer irradiation or higher power resulted in partial decomposition or agglomeration. The resulting precipitate was centrifuged and washed with distilled water. The washing process was repeated 3 to 5 times, and the pH of the washing solution was checked after each cycle using pH indicator strips and confirmed with a pH meter (Ohaus) until a neutral pH (7.0 ± 0.5) was achieved. The precipitate was then dried in an oven at 60°C for 24 hours. To obtain HA with high crystallinity, variations in the EDTA:Ca composition were carried out (Table 1).

Table 1. Variation of EDTA:Ca ratio in HA synthesis

Component	Treatment		
	1	2	3
EDTA:Ca (mol)	0.75:1	0.5:1	0.25:1
pH	13	13	13
Volume (mL)	100	100	100

2.3. Extraction of Avocado Seed

Avocado seeds were washed, cut into small pieces, air-dried, and ground into a fine powder. The powder was macerated in 70% ethanol for 24 hours, followed by filtration. This extraction process was repeated three times. The combined filtrate was evaporated to obtain a concentrated avocado seed extract.

2.4. Toothpaste Formulation

The toothpaste formulation (Table 2) was prepared based on the method reported by Rarung et al. (2022) CMC-Na was dispersed in hot distilled water and allowed to hydrate for 15 minutes, followed by homogenization. Sodium saccharin and sodium benzoate were dissolved separately and mixed into the CMC dispersion. Glycerin and menthol were then added under continuous stirring.

Hydroxyapatite and avocado seed (powder or extract) were incorporated gradually according to the formulation composition. Sodium lauryl sulfate (SLS) was added as a surfactant. The mixture was then homogenized using a homogenizer at 8000 rpm for approximately 10–15 minutes at room temperature to ensure uniform dispersion of all components.

2.5. Characterization of Hydroxyapatite

The synthesized HA was characterized using X-ray diffraction (XRD, Bruker D8 Advance) to determine phase composition and crystallinity, Fourier transform infrared spectroscopy (FTIR) to identify functional groups Scanning electron microscopy (SEM) for morphology analysis.

Table 2. Composition of toothpaste formulations (F1–F9)

Component	Use	F1	F2	F3	F4	F5	F6	F7	F8	F9
$CaCO_3$	Abrasive agent	40	-	-	-	-	-	-	-	-
HA	Active ingredient	-	40	30	20	10	40	40	50	50
Avocado seed powder	Active ingredient	-	-	5	10	15	-	-	-	-
Avocado seed extract	Active ingredient	-	-	-	-	-	5	10	5	10
Na CMC	Binding agent	1	1	1	1	1	1	1	1	1
Glycerin	Humectant	30	30	30	30	30	30	30	30	30
SLS (Sodium Lauryl Sulfate)	Surfactant	1.5	1.5	1.5	1.5	1.5	1.5	1.5	1.5	1.5
Sodium benzoate	Preservative	0.1	0.1	0.1	0.1	0.1	0.1	0.1	0.1	0.1
Sodium saccharin	Sweetener	0.2	0.2	0.2	0.2	0.2	0.2	0.2	0.2	0.2
Distilled water	Solvent	qs	qs	qs	qs	qs	qs	qs	qs	qs
Total		100	100	100	100	100	100	100	100	100

Note: F1 (C40); F2 (HA40); F3 (HA30-B5); F4 (HA20-B10); F5 (HA10-B15); F6 (HA40-E5); F7 (HA40-E10); F8 (HA50-E5); F9 (HA50-E10)

2.6. Physicochemical Evaluation of Toothpaste

2.6.1. Organoleptic Test

Organoleptic properties including color, odor, and physical appearance were evaluated through direct observation (Nofriyanti & Lini, 2021).

2.6.2. pH Measurement

The pH of toothpaste samples was measured using a pH meter after dilution with deionized water. The acceptable pH range follows SNI standards (4.5–10.5) (Nikfallah et al., 2023).

2.6.3. Foam Stability

Foam stability was evaluated by dispersing 1 g of sample in 100 mL of distilled water and shaking for 20 seconds. Foam height was recorded immediately and after 5 minutes. Foam stability (%) was calculated using:

$$\%\ foam\ stability = \frac{initial\ foam\ height}{final\ foam\ height}\ x\ 100\%$$

(Aras & Fia Lestari, 2024)

2.6.4. Spreadability

Spreadability was determined by placing 0.5 g of toothpaste between two glass plates and applying a 150 g load for 5 minutes. The diameter was measured and averaged. Acceptable spreadability ranges from 2.61 to 5.32 cm (Gratia et al., 2021). Unless otherwise stated, all physicochemical measurements were performed in triplicate and the results are presented as mean ± standard deviation.

2.7. Antibacterial Activity

The antibacterial activity of the toothpaste formulations was tested against Streptococcus mutans ATCC 25125 using the agar disc diffusion method. The bacterial suspension was adjusted to 0.5 McFarland standard (approximately 1.5×10^8 CFU/mL) and swabbed evenly onto Mueller-Hinton agar plates. A total of 20 µL of each toothpaste formulation was applied to sterile paper discs (6 mm diameter). The discs were then placed onto the inoculated agar plates. All experiments were performed in duplicate (n=2) for each formulation, except for formulation F3 pre-storage, which was tested in triplicate (n=3). The plates were incubated at 37°C for 24 hours, after which the zones of inhibition were measured in millimeters. Antibacterial assays were performed in triplicate for each formulation. The inhibition zone diameter was expressed as the mean value obtained from three independent measurements.

3. Result and Discussion

3.1. Synthesis and Characterization of Hydroxyapatite (HA)

To valorize chicken eggshells as a calcium precursor, raw eggshell-derived $CaCO_3$ was characterized by XRF, followed by microwave-assisted synthesis of hydroxyapatite (HA). The resulting HA was characterized for crystal structure, functional groups, and morphology to confirm HA formation and evaluate its suitability for toothpaste applications.

3.1.1. Characterization of $CaCO_3$ as HA Precursor

Chicken eggshells are an abundant natural calcium source, composed primarily of calcium carbonate ($CaCO_3$, 92–97 wt%), along with minor amounts of calcium phosphate (~1%), organic matter (~4%), and magnesium carbonate (~1%) (Harisaeng et al., 2025; Kareem & Eyiler, 2024). The eggshell consists of three main layers: the outer cuticle (~10 μm), the palisade layer (~100 μm), and the inner mammillary layer, followed by organic-rich membranes (Owuamanam & Cree, 2020). Residual organic matter can inhibit nucleation or introduce impurities during HA synthesis; therefore, removal of the inner membranes is a crucial purification step. After cleaning, the eggshells were ground using a planetary ball mill and sieved through a 100-mesh sieve to achieve uniform particle size, which increases surface area and improves dissolution, reactivity, and controlled nucleation during HA formation.

Table 3. Elemental composition of chicken eggshell determined by XRF

Elements	%mass
Ca	88.78
Al	4.65
Na	3.69
Mg	2.12

The XRF analysis presented in Table 3 shows that calcium is the dominant element in the chicken eggshell precursor, accounting for 88.78 wt%. This high calcium content confirms that chicken eggshells are a suitable calcium source for hydroxyapatite (HA) synthesis. In addition to calcium, minor amounts of aluminum (Al), sodium (Na), and magnesium (Mg) were also detected. The presence of these elements indicates that the eggshell precursor is not entirely composed of pure $CaCO_3$, which is consistent with the natural composition of biological materials. Nevertheless, the relatively high proportion of calcium compared to the other detected elements suggests that the eggshell can provide sufficient calcium for HA formation. The identification and quantification of calcium are particularly important because they provide essential information for determining the amount of phosphate precursor required during synthesis and for controlling the stoichiometric composition of the final HA product.

Importantly, the measured calcium content was used as the basis for calculating the Ca/P molar ratio in the synthesis process. This step is crucial because deviations from the stoichiometric Ca/P ratio of 1.67 can lead to the formation of secondary phases such as tricalcium phosphate (TCP) or residual $CaCO_3$, thereby affecting the crystallinity and bioactivity of HA.

3.1.2. Microwave-Assisted Synthesis of Hydroxyapatite

Hydroxyapatite was synthesized using a microwave-assisted method with a Ca/P molar ratio of 1.67 by reacting $CaCO_3$ with diammonium hydrogen phosphate (DHP) in the presence of EDTA as a complexing agent. The reaction mixture was prepared in carbonate-free distilled water to minimize unwanted carbonate incorporation. The use of microwave irradiation offers several advantages over conventional hydrothermal methods, particularly in terms of rapid and uniform volumetric heating. Unlike conventional heating, which relies on heat transfer from the surface, microwave energy directly interacts with polar molecules and ionic species, resulting in faster nucleation kinetics and reduced synthesis time. This rapid energy transfer can promote the formation of smaller crystallites and potentially enhance phase purity, although it may also limit complete phase transformation if the irradiation conditions are insufficient.

The reaction pH was adjusted to 13 using 5 M NaOH, which plays a crucial role in HA formation. At highly alkaline conditions, phosphate species predominantly exist as PO_4^{3-}, which is essential for HA precipitation. Additionally, high pH promotes deprotonation of EDTA, enabling it to act effectively as a hexadentate ligand. The reaction mechanism begins with the dissolution of $CaCO_3$ through complexation with EDTA:

$$CaCO_3 + EDTA^{4-} \rightarrow Ca\text{–}EDTA^{2-} + CO \quad (1)$$

EDTA stabilizes Ca^{2+} ions in solution by forming a Ca–EDTA complex, effectively controlling the release rate of free calcium ions. This controlled release is critical in regulating nucleation and preventing uncontrolled precipitation. Upon addition of phosphate ions, Ca^{2+} is gradually released from the complex and reacts to form calcium phosphate nuclei.

Under microwave irradiation, these nuclei rapidly grow into HA crystallites. However, the growth process is influenced by both the stability of the Ca–EDTA complex and the adsorption of OH^- ions on the crystal surface. At pH 13, the high concentration of OH^- ions leads to uniform adsorption across crystal planes, which can limit anisotropic growth and result in more isotropic particle morphology (Liu et al., 2004). Three samples were prepared with different EDTA:Ca molar ratios, namely HA1 (0.75:1), HA2 (0.5:1), and HA3 (0.25:1). This variation is critical because EDTA concentration directly affects the balance between nucleation and crystal growth. Excessive EDTA may overly stabilize Ca^{2+}, slowing nucleation, whereas insufficient EDTA may lead to rapid precipitation and poor crystallinity.

3.1.3. Crystal Structure and Phase Analysis by XRD

X-ray diffraction (XRD) analysis was conducted to identify the crystalline phases and structural characteristics of the synthesized HA. Hydroxyapatite possesses the chemical formula $Ca_{10}(PO_4)_6(OH)_2$ and crystallizes in a hexagonal structure belonging to the $P6_3/m$ space group. This crystal structure is characterized by phosphate tetrahedra and hydroxyl channels that contribute to its excellent biocompatibility, bioactivity, and enamel remineralization capability. The diffraction patterns were recorded in the 2θ range of 2°–80° using Cu Kα radiation (λ = 1.54060 Å), and phase identification was performed using the ICDD database. The XRD patterns (Figure 2) reveal that all samples contain two phases: hydroxyapatite (HA) and calcite ($CaCO_3$). The presence of characteristic HA peaks at 2θ ≈ 25.87°, 31.77°, and 32.2°, corresponding to the (002), (121), and (112) planes, confirms the successful formation of HA.

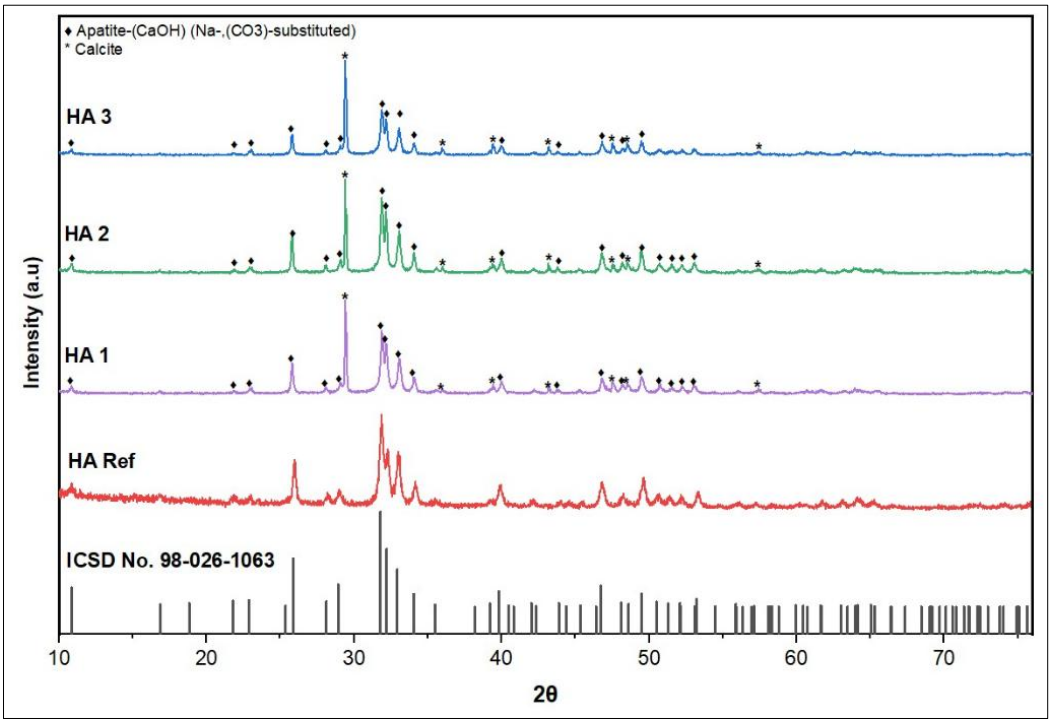

Figure 2. XRD patterns of HA samples at different EDTA:Ca ratios compared with reference HA (ICSD No. 98-026-1063)

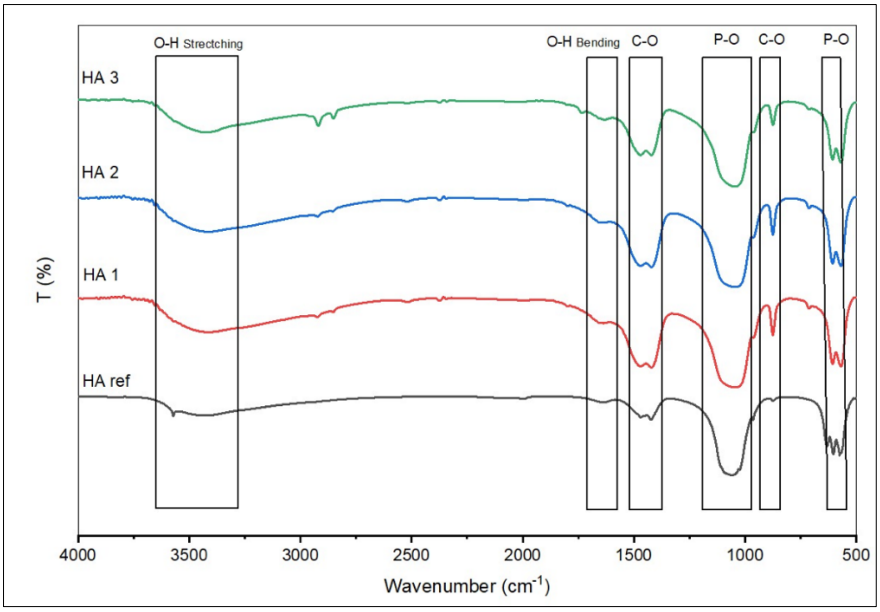

Figure 3. FTIR spectra of HA samples at different EDTA:Ca ratios compared with reference HA

However, the simultaneous presence of calcite peaks indicates incomplete conversion of $CaCO_3$ into HA. This suggests that the synthesis conditions were not fully optimized. A key factor contributing to this incomplete conversion is the absence of a calcination step, which is typically required to enhance $CaCO_3$ reactivity and facilitate phase transformation. Additionally, the relatively moderate microwave power (450 W) and limited irradiation time may have restricted the extent of the reaction. This observation aligns with previous studies indicating that higher temperatures and longer reaction times promote the complete transformation of $CaCO_3$ into HA (Fitriyana et al., 2025). Therefore, while microwave-assisted synthesis offers rapid processing, it may require optimization of power and duration to achieve higher phase purity.

Table 4. Weight percentage (wt%) of crystalline phases based on Rietveld refinement

Sample	Apatite (%)	Calcite (%)
HA 1	81.3	18.7
HA 2	82.5	17.5
HA 3	70.5	29.5

Quantitative phase analysis (Table 4) shows that HA2 (EDTA:Ca = 0.5:1) exhibits the highest HA content (82.5 wt%), whereas HA3 shows the lowest (70.5 wt%). This indicates that an intermediate EDTA concentration provides the optimal balance between calcium complexation and release, facilitating more efficient HA formation. The presence of residual calcite indicates that the conversion of $CaCO_3$ into hydroxyapatite was not complete under the selected synthesis conditions.

The absence of a calcination step was intentional and aligned with the objective of developing a low-energy, one-pot microwave-assisted synthesis route. Calcination typically requires temperatures above 700–900 °C, resulting in increased energy consumption and processing costs. From a sustainability perspective, the present approach is consistent with Green Chemistry principles by reducing thermal treatment requirements. Moreover, the residual calcite phase may not be entirely detrimental for toothpaste applications because calcium carbonate is commonly employed as a mild abrasive in commercial dentifrices. Therefore, the remaining calcite could potentially contribute additional polishing functionality while maintaining biocompatibility.

Nevertheless, further optimization of microwave irradiation parameters or post-synthesis treatment may further improve the hydroxyapatite purity when applications requiring highly phase-pure HA are targeted.

In particular, adjusting the irradiation time and microwave power may promote a more complete conversion of calcite into HA, thereby enhancing the phase purity of the synthesized material.

Table 5. Degree of crystallinity of HA samples

Sample (Ratio)	Crystall -ine Area	Total Area (Crystalline and Amorphous)	Degree of Crystallinity (%)
1 (0.75:1)	2505.46	3124.88	80.18
2 (0.50:1)	2465.58	3151.89	78.23
3 (0.25:1)	2392.70	3207.92	74.59

The crystallinity data (Table 5) further demonstrate that increasing EDTA concentration generally enhances crystallinity. This can be attributed to the role of EDTA in moderating nucleation rates and allowing more ordered crystal growth. However, excessive EDTA may also slow down the reaction kinetics, indicating the need for an optimal balance. Overall, these results highlight that the EDTA:Ca ratio is a critical parameter influencing both phase composition and crystallinity. The HA2 sample (0.5:1) appears to provide the most favorable conditions for producing high-quality HA.

3.1.4. Functional Group Identification of Hydroxyapatite

Fourier Transform Infrared (FTIR) spectroscopy was employed to identify the functional groups present in the synthesized HA samples and to further validate phase formation at the molecular level. While XRD confirms crystallographic phases, FTIR provides complementary information regarding bonding environments and possible ionic substitutions within the HA structure. The characteristic FTIR bands observed in this study are consistent with the molecular structure of hydroxyapatite, $Ca_{10}(PO_4)_6(OH)_2$, which contains phosphate (PO_4^{3-}) groups as the primary structural framework and hydroxyl (OH^-) groups located along the crystallographic c-axis. The FTIR spectra (Figure 3 and Table 6) show several characteristic absorption bands associated with hydroxyapatite. A broad band observed in the range of 3500–3000 cm^{-1} corresponds to the stretching vibration of hydroxyl (O–H) groups, which are essential components of the HA lattice. The presence of this band confirms the incorporation of structural hydroxyl groups, although its broad nature also suggests possible contributions from adsorbed water molecules on the particle surface.

Table 6. Summary of FTIR wavenumbers and corresponding functional groups

Sample Wavenumber (cm-1)	Reference Wavenumber (cm-1)	Functional group	Vibration mode	Reference
3500–3000	3700 – 2600	O-H	Stretching	(Zhou & Lee, 2011)
1460	1460 dan 1414	C-O	Stretching	(Vinoth Kumar et al., 2021)
875	870	C-O	Stretching	(Wang et al., 2021)
1100–900	1016 dan 1027	P-O	Asimetris stretching	(Sabu et al., 2019)
600	603	P-O	Bending	(Abifarin et al., 2019)

The phosphate group (PO_4^{3-}), which constitutes the backbone of HA, is clearly identified by strong absorption bands in the region of 1100–900 cm^{-1}, corresponding to the asymmetric stretching vibration (ν_3). Additionally, the bending vibration (ν_4) of phosphate appears around 600–560 cm^{-1} (specifically at 604 cm^{-1} and 565 cm^{-1}). The intensity and sharpness of these bands are indicative of the degree of structural ordering, where more defined peaks suggest higher crystallinity. Across the three samples (F1, F2, F3), subtle shifts and intensity variations in the phosphate bands were observed. For instance, the splitting of the ν_4 bending mode became more pronounced from F1 to F3, suggesting

an increase in crystallinity that correlates with the XRD results.

Carbonate-related bands are observed at approximately 1460 cm^{-1} and 875 cm^{-1}, corresponding to asymmetric stretching (ν_3) and out-of-plane bending vibrations of CO_3^{2-}, respectively. To determine whether these carbonate bands originate from lattice substitution or residual unreacted $CaCO_3$.

Importantly, the presence of carbonate bands at 1460 cm^{-1} and 875 cm^{-1}, without a distinct band near 1540 cm^{-1} (characteristic of A-type substitution, where CO_3^{2-} replaces OH^-), confirms B-type carbonate substitution (CO_3^{2-} replacing PO_4^{3-}) as the predominant substitution mechanism. This distinction has important functional implications: B-type substitution is known to increase the bioactivity and solubility of HA compared to stoichiometric HA, which is beneficial for remineralization applications in toothpaste formulations (Madupalli et al, 2017).

Across the three samples, slight variations in the relative intensity of the carbonate bands were observed. For example, the band at 1460 cm^{-1} showed a gradual decrease in relative intensity from F1 to F3, suggesting a lower degree of carbonate substitution in F3. These differences correlate with the observed variations in crystallinity and solubility discussed later. The presence of carbonate groups, as confirmed by FTIR, is consistent with the XRD results which detected calcite as a secondary phase, although FTIR confirms that most carbonate is incorporated into the HA lattice rather than remaining as free calcite.

This reinforces the need for optimizing synthesis conditions to minimize unwanted carbonate phases while maintaining desirable bioactive properties.

3.1.5. Morphological Analysis of Hydroxyapatite

The morphology and surface characteristics of the synthesized HA were analyzed using scanning electron microscopy (SEM). Morphological features play a significant role in determining the material's reactivity, surface area, and interaction with biological systems, particularly for dental applications.

The SEM images (Figure 4) reveal that the synthesized HA particles are predominantly in the nanoscale range with irregular shapes. The particles exhibit a tendency to form aggregates, where smaller primary particles cluster into larger agglomerates. This agglomeration behavior is commonly observed in nanoparticle systems due to high surface energy, which drives particles to reduce their total surface area through aggregation.

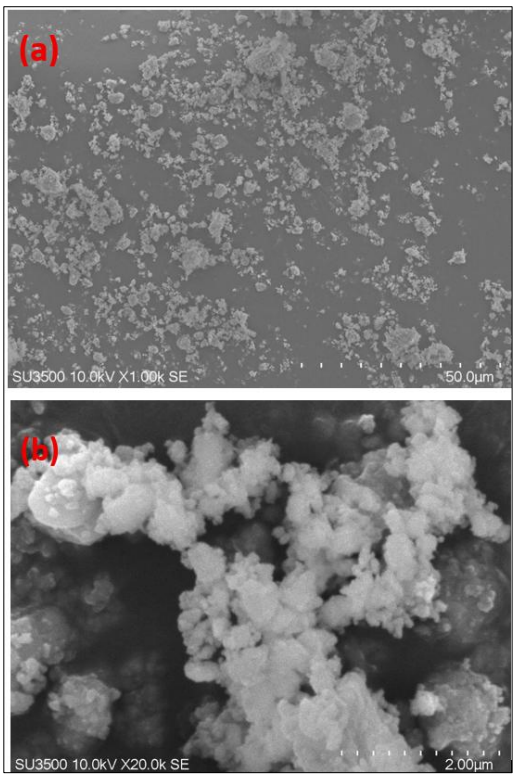

Figure 4. SEM images of HA2 (EDTA:Ca = 0.5:1) at (a) 1,000× and (b) 20,000× magnifications

The irregular morphology suggests that crystal growth occurred in a relatively uncontrolled manner, likely influenced by rapid nucleation under microwave irradiation. While microwave-assisted synthesis promotes fast formation of nuclei, it can also limit the time available for directional crystal growth, resulting in non-uniform particle shapes. Additionally, the presence of agglomerates

indicates strong interparticle interactions, possibly driven by van der Waals forces or residual surface charges. This phenomenon may also be influenced by the absence of dispersing agents or post-synthesis treatments such as ultrasonication.

Particle size analysis using ImageJ indicates a relatively broad size distribution, suggesting that the system lacks uniformity in nucleation and growth processes. This heterogeneity may impact the consistency of HA performance, particularly in applications where uniform particle size is desirable. From an application perspective, nanoscale HA is advantageous due to its higher surface area and enhanced reactivity, which can improve its interaction with tooth enamel. However, excessive agglomeration may reduce the effective surface area and limit its functional performance. Therefore, further optimization such as controlling synthesis parameters or introducing dispersing strategies is necessary to achieve more uniform morphology and particle distribution.

3.2. Formulation and Physical Characteristics of Hydroxyapatite-Based Toothpaste Enriched with Avocado Seed

Hydroxyapatite (HA) and avocado seed were selected as the main active components due to their complementary functions. HA is a bioactive inorganic material that promotes remineralization and protects against dental caries, dentin hypersensitivity, and enamel degradation (Chen et al., 2021). Meanwhile, avocado seed contains phenolic compounds (flavonoids and tannins), as well as alkaloids and saponins, which exhibit antibacterial activity by disrupting bacterial cell walls and membranes (Beby et al., 2023). Therefore, the combination of HA and avocado seed is expected to provide both mechanical protection and biological activity. In the control formulation (F1), calcium carbonate (40%) was used as the abrasive agent to remove stains and dental plaque. In formulations F2–F9, $CaCO_3$ was partially or completely replaced with HA to evaluate its function as both an abrasive and a remineralizing bioactive agent.

Unlike conventional abrasives, HA offers additional benefits, including the ability to form a protective mineral layer on the tooth surface and potentially inhibit bacterial adhesion. This substitution is therefore not merely compositional but functional, aiming to enhance the therapeutic value of the toothpaste. Sodium lauryl sulfate (SLS) was incorporated as a surfactant at a concentration of 1.5% to reduce surface tension and facilitate the removal of debris. SLS is known for its effective foaming properties and stability, even in the presence of ions, although its interaction with calcium-containing compounds may influence foam stability.

Glycerin was used as a humectant (30%) to retain moisture and prevent drying of the formulation. Humectants are essential in maintaining the physical stability and usability of toothpaste during storage. Sodium saccharin and menthol were added as flavoring agents to improve consumer acceptability, providing sweetness and a cooling sensation, respectively. Sodium carboxymethyl cellulose (Na-CMC) was used as a binder to ensure homogeneity and maintain the consistency of the formulation. As a hydrophilic polymer, Na-CMC forms a gel-like structure that stabilizes the dispersion of solid particles within the paste. Sodium benzoate was included as a preservative to inhibit microbial growth and ensure product stability during storage. Its effectiveness depends on concentration and formulation conditions, particularly pH.

Overall, the formulation strategy in this study is designed to balance mechanical, chemical, and biological functions. The substitution of $CaCO_3$ with HA and the incorporation of avocado seed derivatives represent a functional modification aimed at enhancing both the performance and bioactivity of the toothpaste.

3.2.1. Organoleptic Evaluation of Toothpaste Formulations

Organoleptic evaluation assessed the consistency, color, aroma, and taste of the formulations over 21 days of storage (Table 7,8,9). All formulations remained semi-solid

throughout, indicating acceptable physical stability. However, viscosity varied across formulations. The commercial control (X) and F1–F7 showed consistent viscous texture, while F8 and F9 exhibited increased thickness, with F9 being highly viscous from day one.

This variation correlates strongly with solid component concentration, particularly HA and avocado seed powder. Higher solid loading increases internal flow resistance, leading to greater viscosity. Thus, the rheological behavior is governed primarily by the solid-to-liquid ratio rather than the constant binder concentration.

Table 7. Evaluation of physical consistency (viscosity/texture) of the toothpaste formulations

Formula	Day of Observation			
	0	7	14	21
X (Commercial)	+	+	+	+
F1 (C40)	+	+	+	+
F2 (HA40)	+	+	+	+
F3 (HA30-B5)	+	+	+	+
F4 (HA20-B10)	+	+	+	+
F5 (HA10-B15)	+	+	+	+
F6 (HA40-E5)	+	+	+	+
F7 (HA40-E10)	+	+	+	+
F8 (HA50-E5)	+	+	++	++
F9 (HA50-E10)	++	++	++	++

*(C) $CaCO_3$; (HA) Hydroxyapatite; (B) Avocado seed powder; (E)Avocado seed extract; (+) Thick consistency; (++) Highly viscous / Very thick consistency

Table 8. Evaluation of color of the toothpaste formulations

Formula	Day of Observation			
	0	7	14	21
X (Kormersial)	White	White	White	White
F1 (C40)	White	White	White	White
F2 (HA40)	White	White	White	White
F3 (HA30-B5)	Light brown	Light brown	Light brown	Light brown
F4 (HA20-B10)	Brown	Brown	Brown	Dark brown
F5 (HA10-B15)	Brown	Brown	Dark brown	Dark brown
F6 (HA40-E5)	Light brown	Light brown	Light brown	Light brown
F7 (HA40-E10)	Light brown	Light brown	Light brown	Light brown
F8 (HA50-E5)	Light brown	Light brown	Light brown	Light brown
F9 (HA50-E10)	Light brown	Light brown	Light brown	Light brown

*(C) $CaCO_3$; (HA) Hydroxyapatite; (B) Avocado seed powder; (E) Avocado seed extract

Table 9. Evaluation of smell of the toothpaste formulations of taste

Formula	Day of Observation			
	0	7	14	21
X (Kormersial)	M	M	M	M
F1 (C40)	M	M	M	M
F2 (HA40)	M	M	M	M
F3 (HA30-B5)	SBA	SBA	SBA	SBA
F4 (HA20-B10)	SBA	SBA	SBA	SBA
F5 (HA10-B15)	SBA	SBA	SBA	SBA
F6 (HA40-E5)	SBA	SBA	SBA	SBA
F7 (HA40-E10)	SBA	SBA	SBA	SBA
F8 (HA50-E5)	SBA	SBA	SBA	SBA
F9 (HA50-E10)	SBA	SBA	SBA	SBA

*(C) $CaCO_3$; HA: Hydroxyapatite; (B)Avocado seed powder; (E)Avocado seed extract; (M) Menthol; (SAB) Specific avocado seed aroma

Color observations showed that formulations without avocado seed (X, F1, F2) remained white, whereas those containing avocado seed displayed varying shades of brown. The darker color in F4 and F5 was associated with higher avocado seed concentrations, likely due to oxidation of phenolic compounds. Slight darkening during storage suggests continued oxidation or polymerization of these compounds. Although the change was not significant, it indicates that antioxidant stabilization may be needed to preserve the visual quality of formulations containing plant-derived ingredients throughout shelf life.

Aroma evaluation indicated that menthol-dominated formulations (X, F1, F2) maintained a stable scent profile, whereas formulations containing avocado seed exhibited a characteristic plant-like odor. The persistence of this aroma throughout storage suggests minimal volatilization or degradation of aromatic compounds. From a formulation perspective, this finding indicates that the menthol concentration may be insufficient to fully mask the intrinsic odor of avocado seed, which could negatively influence consumer acceptance.

Taste evaluation showed that formulations X, F1, and F2 maintained a sweet profile, while formulations containing avocado seed ranged from slightly sweet to slightly bitter. The bitterness observed in F5 was particularly notable and correlated with the highest concentration of avocado seed powder. This bitterness is likely attributable to phenolic compounds and other bioactive constituents present in the avocado seed, which may impart a bitter taste at higher loadings. These organoleptic limitations should be considered when optimizing the formulation for consumer acceptability.

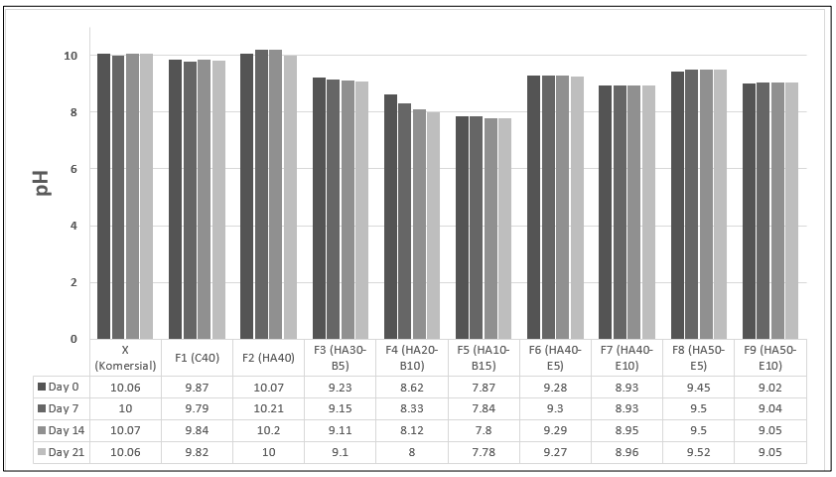

	X (Komersial)	F1 (C40)	F2 (HA40)	F3 (HA30-B5)	F4 (HA20-B10)	F5 (HA10-B15)	F6 (HA40-E5)	F7 (HA40-E10)	F8 (HA50-E5)	F9 (HA50-E10)
Day 0	10.06	9.87	10.07	9.23	8.62	7.87	9.28	8.93	9.45	9.02
Day 7	10	9.79	10.21	9.15	8.33	7.84	9.3	8.93	9.5	9.04
Day 14	10.07	9.84	10.2	9.11	8.12	7.8	9.29	8.95	9.5	9.05
Day 21	10.06	9.82	10	9.1	8	7.78	9.27	8.96	9.52	9.05

Figure 5. Effect of formulation variation on pH over storage time

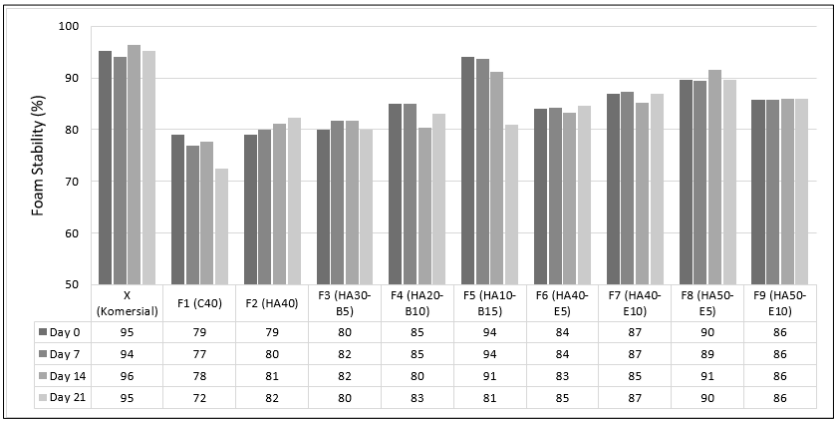

	X (Komersial)	F1 (C40)	F2 (HA40)	F3 (HA30-B5)	F4 (HA20-B10)	F5 (HA10-B15)	F6 (HA40-E5)	F7 (HA40-E10)	F8 (HA50-E5)	F9 (HA50-E10)
Day 0	95	79	79	80	85	94	84	87	90	86
Day 7	94	77	80	82	85	94	84	87	89	86
Day 14	96	78	81	82	80	91	83	85	91	86
Day 21	95	72	82	80	83	81	85	87	90	86

Figure 6. Effect of formulation variation on foam stability (%)

This suggests that phenolic compounds, especially tannins, contribute significantly to taste perception. Importantly, this highlights a formulation trade-off: increasing bioactive content may enhance antibacterial potential but reduce sensory acceptability.

3.2.2. pH Evaluation of Toothpaste Formulations

The pH of toothpaste is a critical parameter influencing both product safety and compatibility with the oral environment. Ideally, toothpaste should exhibit a neutral to slightly alkaline pH to prevent mucosal irritation while preserving its protective effects on dental enamel. According to ISO 11609 and previously reported toothpaste formulations, the acceptable pH range for dentifrices generally lies between 4.5 and 10.5, ensuring product safety while minimizing the risk of enamel erosion and oral mucosal irritation. The results showed (see Figure 5) that all formulations fell within the acceptable pH range of 4.5–10.5, with most displaying alkaline characteristics. The commercial toothpaste (X) maintained a stable pH of approximately 10, and the HA-containing formulations (e.g., F2) exhibited comparable behavior. This behavior is attributed to the buffering capacity of hydroxyapatite (HA). Under acidic conditions, HA partially dissolves, releasing Ca^{2+} ions that help stabilize pH and support enamel remineralization.

A decreasing trend in pH is observed with increasing avocado seed content. This is likely due to the presence of phenolic compounds, which can contribute to a more acidic environment. However, the overall pH remains within acceptable limits, suggesting that HA effectively counterbalances the acidity introduced by plant extracts. This interplay between HA and avocado seed demonstrates a functional buffering system within the formulation, where inorganic and organic components collectively influence pH stability.

3.2.3. Foam Stability of Toothpaste Formulations

All formulations exhibited foam stability within the range of approximately 72.4–94.1%, indicating relatively stable foaming behavior (Figure 6). However, notable variations exist between formulations. F1 showed the lowest foam stability, which may be attributed to the presence of $CaCO_3$. In contrast, formulations containing HA exhibited moderate to high foam stability, although slightly lower than the commercial control.

This behavior can be explained by the interaction between surfactants (SLS) and divalent cations such as Ca^{2+}. HA surfaces can adsorb Ca^{2+} ions, which may interact with surfactant molecules and reduce their availability for foam formation. This phenomenon is analogous to the effect observed in hard water, where Ca^{2+} and Mg^{2+} reduce surfactant efficiency.

On the other hand, avocado seed contains saponins, which act as natural surfactants and contribute to foam formation. This explains why certain formulations (e.g., F4 and F8) exhibit relatively higher foam stability despite containing HA. However, excessive solid content, particularly from avocado seed powder, may hinder foam formation by increasing viscosity and limiting bubble expansion. This explains the fluctuation observed in formulations with higher solid loading.

3.2.4. Spreadability of Toothpaste Formulations

All formulations fall within the acceptable spreadability range (2.61–5.32 cm), indicating suitable application properties (Figure 7). However, clear trends are observed. Formulations X and F1 exhibit the highest spreadability, likely due to lower viscosity and reduced solid content. In contrast, F2 shows the lowest spreadability, indicating a more viscous system. A general decrease in spreadability is observed with increasing HA concentration, which can be attributed to higher solid loading and increased resistance to flow. This is consistent with rheological principles, where increased particle interactions lead to higher viscosity and reduced flowability.

Formulations containing avocado seed powder also show reduced spreadability over time. This may be due to the presence of starch and polysaccharides, which can absorb water and increase viscosity during storage. Interestingly, formulations containing avocado seed extract (F6–F9) show more stable spreadability compared to powder-based formulations. This suggests that extract-based systems provide better physical stability due to reduced solid content and more uniform dispersion.

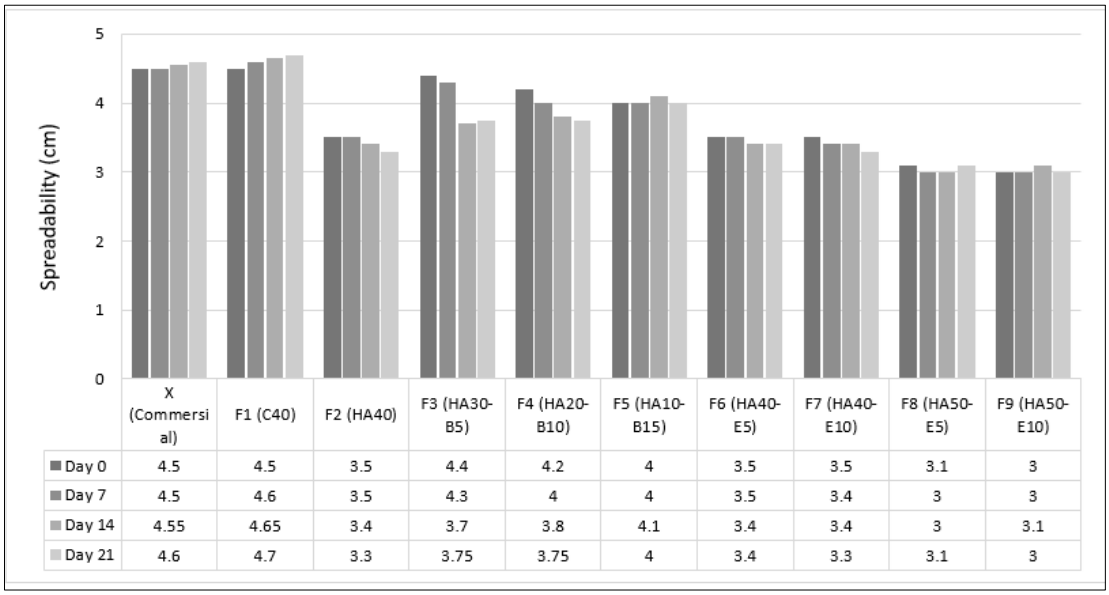

	X (Commersial)	F1 (C40)	F2 (HA40)	F3 (HA30-B5)	F4 (HA20-B10)	F5 (HA10-B15)	F6 (HA40-E5)	F7 (HA40-E10)	F8 (HA50-E5)	F9 (HA50-E10)
Day 0	4.5	4.5	3.5	4.4	4.2	4	3.5	3.5	3.1	3
Day 7	4.5	4.6	3.5	4.3	4	4	3.5	3.4	3	3
Day 14	4.55	4.65	3.4	3.7	3.8	4.1	3.4	3.4	3	3.1
Day 21	4.6	4.7	3.3	3.75	3.75	4	3.4	3.3	3.1	3

Figure 7. Effect of formulation variation on spreadability (cm)

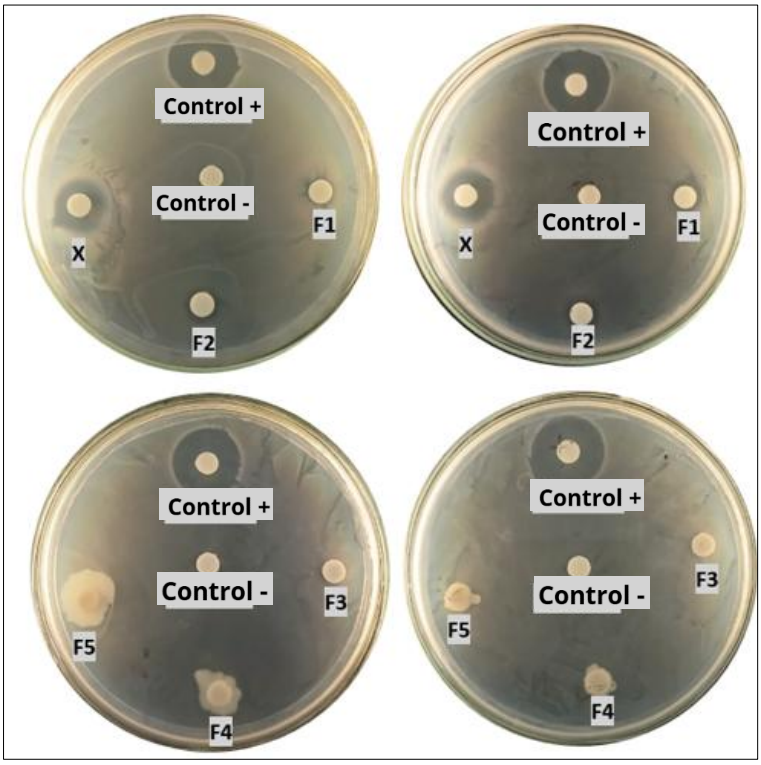

Figure 8. Documentation of antibacterial activity testing of HA and avocado seed powder toothpaste against Streptococcus mutans ATCC 25125 after 30 days of storage

Table 10. Antibacterial activity of HA and avocado seed powder toothpaste against Streptococcus mutans ATCC 25125 after 30 days of storage

Samle	Antibacterial Inhibition Zone Diameter (mm)		Mean (mm)
	I	II	
Control (-)	≤6	≤6	≤6
Control (+)	20.0	20.0	20.0
X (Commersial)	14.8	16.4	15.6
F1(C40)	7.1	9	8.05
F2 (HA40)	10.2	9.4	9.8
F3 (H30-B5)	≤6	≤6	≤6
F4 (HA20-B10)	-	-	-
F5 (HA10-B15)	-	-	-

*Positive control: 0.2% Chlorhexidine; Negative control: Sample solvent (distilled water); Disc diameter: 6 mm; A value of 6 mm indicates no inhibition zone (diameter equal to the disc size); F4 and F5 were excluded from measurement due to contamination

3.3. Antibacterial Activity Against Streptococcus mutans

After 30 days of storage, the commercial toothpaste exhibited strong antibacterial activity (15.6 mm), while F1 and F2 showed moderate activity (8.05 mm and 9.8 mm, respectively). The antibacterial mechanism of HA is not fully understood but is suggested to involve disruption of bacterial metabolism and possible generation of reactive species during synthesis (see Figure 8 and Table 10).

Notably, formulations containing avocado seed powder (F3–F5) showed poor or no activity after storage, with F4 and F5 exhibiting contamination. This indicates a significant limitation in microbiological stability when using raw plant powder. This instability is likely due to the presence of nutrients (e.g., carbohydrates and proteins) that support microbial growth, as well as the hygroscopic nature of the powder, which promotes moisture retention. During storage, formulations F4 and F5 (containing avocado seed extract) showed visible signs of contamination, whereas F1–F3 (containing avocado seed powder) remained stable. Microscopic examination revealed filamentous structures consistent with fungal growth.

The contamination was traced to the avocado seed extract, which was prepared in-house without terminal sterilization. Unlike synthetic preservatives, the natural antibacterial components of avocado seed extract did not provide sufficient protection against fungal proliferation, particularly in the aqueous environment of the toothpaste base. This finding has important implications: while avocado seed extract offers antibacterial benefits against S. mutans, it is not self-preserving and requires either (1) sterilization (e.g., filtration or autoclaving) prior to incorporation, (2) the addition of an approved preservative system (e.g., sodium benzoate, which was present at low concentration), or (3) the use of the more stable powder form as in F1–F3. Consequently, F4 and F5 were excluded from sensory evaluation, and future studies should include preservative efficacy testing according to pharmacopoeial standards.

Before storage, F3 exhibited a very strong antibacterial effect (37.7 mm), indicating that avocado seed contains highly active antibacterial compounds (see Figure 9 and Table 11). However, the drastic decline after storage highlights a critical issue: bioactivity does not guarantee stability.

In contrast, extract-based formulations (F6–F9) maintained stable antibacterial activity after 30 days, with inhibition zones ranging from 8.78 to 10.09 mm (see Figure 10 and Table 12). F9 exhibited the highest activity, suggesting a synergistic effect between higher HA and extract concentrations. The improved stability of extract-based formulations can be attributed to the removal of non-active components during extraction, resulting in a more concentrated and microbiologically stable product.

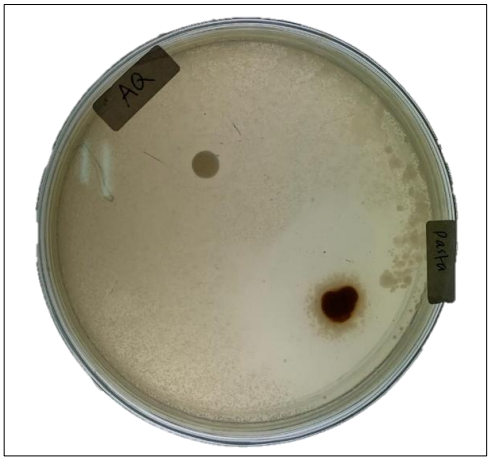

Figure 9. Documentation of antibacterial activity testing for toothpaste formulation F3 (HA30-B5) against Streptococcus mutans ATCC 25125 prior to 30-day storage

The antibacterial activity of avocado seed extract is associated with secondary metabolites such as flavonoids, alkaloids, saponins, and tannins. These compounds act through multiple mechanisms, including membrane disruption, enzyme inhibition, and interference with nucleic acid synthesis. Importantly, the results demonstrate that while powder-based formulations may offer high initial activity, extract-based systems provide better long-term stability and consistent antibacterial performance.

Table 11. Antibacterial activity of toothpaste formulation F3 against Streptococcus mutans ATCC 25125 prior to 30-day storage

Sample	Antibacterial Inhibition Zone Diameter (mm)			Mean (mm)
	I	II	III	
Control (-)	≤6	≤6	≤6	≤6
F3 (HA30-B5)	39.8	31. 7	41.6	37.7

*Negative control: Sample solvent (distilled water)

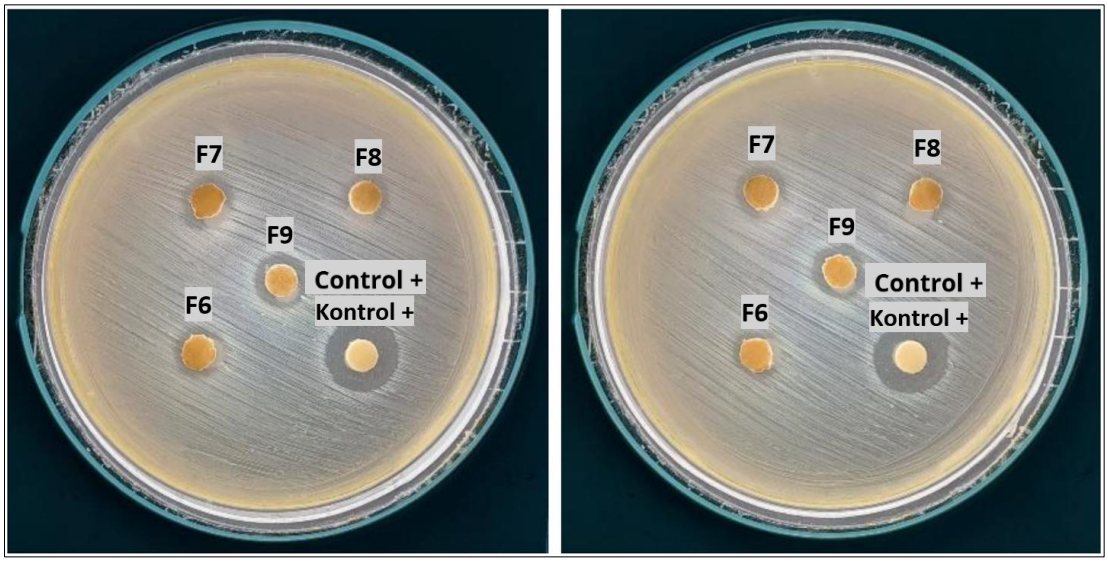

Figure 10. Documentation of antibacterial activity testing of hydroxyapatite (HA) and avocado seed extract toothpaste against Streptococcus mutans ATCC 25125 after 30 days of storage

Table 12. Antibacterial activity of HA and avocado seed extract toothpaste against Streptococcus mutans ATCC 25125 after 30 days of storage

Sample	Antibacterial Inhibition Zone Diameter (mm)		Mean (mm)
	I	II	
Kontrol (+)	13.64	13.74	13.69
F6 (HA40-E5)	8.91	8.64	8.78
F7 (HA40-E10)	9.46	9.81	9.64
F8 (HA50-E5)	8.77	8.93	8.85
F9 (HA50-E10)	9.93	10.24	10.09

*Positive control: 0.2% Chlorhexidin

4. Conclusion

This study successfully demonstrates the feasibility of producing eggshell-derived hydroxyapatite through a microwave-assisted route and incorporating it into antibacterial toothpaste formulations. The synthesized HA had high crystallinity (82.5 wt%), a hexagonal structure, and nanoscale morphology, making it suitable for toothpaste applications. The optimal EDTA:Ca ratio was 0.5:1.

HA-based toothpastes enriched with avocado seed powder and extract showed acceptable physicochemical properties and stability over 21 days. All formulations met standard quality requirements for pH (8.93–10.0), foam stability (72.4–94.1%), and spreadability (3.0–4.7 cm). The results clearly reveal that avocado seed extract provides superior storage stability compared with avocado seed powder. While powder-based formulations exhibited strong initial antibacterial activity, their susceptibility to contamination and bioactivity loss limits their practical application. In contrast, extract-based formulations maintained more consistent antibacterial performance during storage, highlighting their greater potential for oral-care products and bioactive dental materials.

For antibacterial activity against Streptococcus mutans, a key difference was observed between powder and extract formulations. Powder-based formulations showed strong initial activity but lost efficacy after 30 days due to microbial instability. Extract-based formulations, however, maintained stable antibacterial activity over time. Therefore, avocado seed extract is more suitable than powder for stable, long-lasting antibacterial toothpaste. Future studies should evaluate extended storage stability, enamel remineralization performance, preservative optimization, and in vivo efficacy to further validate the applicability of these formulations.

References

Abifarin, J. K., Obada, D. O., & Dauda, E. T. (2019). Experimental data on the characterization of hydroxyapatite synthesized from biowastes. *Data in Brief*, *26*, 104485. https://doi.org/10.1016/j.dib.2019.104485

Anil, A., Ibraheem, W. I., Meshni, A. A., Preethanath, R., & Anil, S. (2022). Demineralization and Remineralization Dynamics and Dental Caries. In L.-C. Rusu & L. C. Ardelean (Eds.), *Dental Caries* (2). IntechOpen. https://doi.org/10.5772/intechopen.105847

Aras, N. R. M., & Fia Lestari, M. (2024). Uji Performa Pengaruh Gliserin dalam Formulasi Sabun Cair Cuci Piring. *Majalah Farmasetika*, *9*(5), 429–442. https://doi.org/10.24198/mfarmasetika.v9i5.56837

Artaningsih, N. L. B., Habibah, N., & Nyoman, M. (2018). Antibacterial activity of ethanol extract of gamal leaves (Gliricidia sepium) at various concentrations on the growth of Streptococcus mutans in vitro. *Jurnal Kesehatan*, *9*(3), 336–345. https://doi.org/10.26630/jk.v9i3.957

Baladi, M., Amiri, M., Mohammadi, P., Salih Mahdi, K., Golshani, Z., Razavi, R., & Salavati-Niasari, M. (2023). Green sol–gel synthesis of hydroxyapatite nanoparticles using lemon extract as capping agent and investigation of its anticancer activity against human cancer cell lines (T98, and SHSY5). *Arabian Journal of Chemistry*, *16*(4), 1–12. https://doi.org/10.1016/j.arabjc.2023.104646

Beby, C. T., Sugiaman, V. K., & Pranata, N. (2023). Comparison of antibacterial activity of both seeds and leaves ethanol extract of avocado (Persea americana Mill.) against Streptococcus mutans Perbandingan aktivitas antibakteri

ekstrak etanol biji dan daun alpukat (Persea americana Mill.) terhadap St. *Makassar Dental Journal*, *12*(1), 38–42. https://doi.org/10.35856/mdj.v12i1.629

Bujung, A. H., Homenta, H., & Khoman, J. A. (2017). Uji daya hambat ekstrak biji buah alpukat (Persea americana Mill.) terhadap pertumbuhan Streptococcus mutans. *E-GIGI*, *5*(2), 112–116. https://doi.org/10.35790/eg.5.2.2017.16535

Castro, M. A. M., Portela, T. O., Correa, G. S., Oliveira, M. M., Rangel, J. H. G., Rodrigues, S. F., & Mercury, J. M. R. (2022). Synthesis of hydroxyapatite by hydrothermal and microwave irradiation methods from biogenic calcium source varying pH and synthesis time. *Boletin de La Sociedad Espanola de Ceramica y Vidrio*, *61*(1), 35–41.https://doi.org/10.1016/j.bsecv.2020.06.003

Chen, L., Al-Bayatee, S., Khurshid, Z., Shavandi, A., Brunton, P., & Ratnayake, J. (2021). Hydroxyapatite in oral care products—A review. *Materials*, *14*(17), 4865. https://doi.org/10.3390/ma14174865

Cocco, F., Salerno, C., Wierichs, R. J., Wolf, T. G., Arghittu, A., Cagetti, M. G., & Campus, G. (2025). Hydroxyapatite-Fluoride Toothpastes on Caries Activity: A Triple-Blind Randomized Clinical Trial. *International Dental Journal*, *75*(2), 632–642. https://doi.org/https://doi.org/10.1016/j.identj.2024.09.037

Daas, I., Badr, S., & Osman, E. (2018). Comparison between fluoride and nano-hydroxyapatite in remineralizing initial enamel lesion: An in vitro study. *Journal of Contemporary Dental Practice*, *19*(3), 306–312. https://doi.org/10.5005/JP-JOURNALS-10024-2258

Djayasinga, R., Situmeang, R. T. M., Unob, F., Hadi, S., Manurung, P., & Sumardi, S. (2024). Chicken Eggshell Powder as Antibacterial of Staphylococcus aureus and Escherichia coli: Invitro. *Journal of Multidisciplinary Applied Natural Science*, *1*(1), 41–46. https://doi.org/10.47352/jmans.2774-3047.205

Fitriyana, D. F., Muhammadin, R. C., Pusparizkita, Y. M., Ismail, R., Jamari, J., & Bayuseno, A. P. (2025). Microwave-assisted synthesis of nanocrystalline hydroxyapatite using calcium supplies from green mussel shells with synthesis time optimization. *Nano-Structures & Nano-Objects*, *42*, 101484. https://doi.org/https://doi.org/10.1016/j.nanoso.2025.101484

Fufa, D. D., Bekele, T., Tamene, A., & Bultosa, G. (2025). Drying kinetic models, thermodynamics, physicochemical qualities, and bioactive compounds of avocado (Persea americana Mill. Hass variety) seeds dried using various drying methods. *Heliyon*, *11*(1), e41058. https://doi.org/10.1016/j.heliyon.2024.e41058

Gratia, B., Yamlean, P. V. Y., & Mansauda, K. L. R. (2021). Formulation of toothpaste of nutmeg ethanol extract (*Myristica fragrans* Houtt.). *Pharmacon*, *10*(3), 968–974. https://doi.org/10.35799/pha.10.2021.35388

Harisaeng, K., Chaikool, P., Mutoh, Y., Chindaprasirt, P., & Laonapakul, T. (2025). Fabrication and characterization of tetra-calcium phosphate from natural wastes of eggshell and cockle shell. *Results in Materials*, *25*, 100670. https://doi.org/10.1016/j.rinma.2025.100670

Hasan, F., Yuliana, L. T., Budi, H. S., Ramasamy, R., Ambiya, Z. I., & Ghaisani, A. M. (2024). Prevalence of dental caries among children in Indonesia: A systematic review and meta-analysis of observational studies. *Heliyon*, *10*(11), e32102. https://doi.org/10.1016/j.heliyon.2024.e32102

Imran, E., Cooper, P. R., Ratnayake, J., Ekambaram, M., & Mei, M. L. (2023). Potential Beneficial Effects of Hydroxyapatite Nanoparticles on Caries Lesions In Vitro—A Review of the Literature. *Dentistry Journal*, *11*(2), 1–24. https://doi.org/10.3390/dj11020040

Irwansyah, F. S., Noviyanti, A. R., Eddy, D. R., & Risdiana, R. (2022). Green template-mediated synthesis of biowaste nano-hydroxyapatite: a systematic literature review. *Molecules*, *27*(17), 5586. https://doi.org/10.3390/molecules27175586

Kareem, Z., & Eyiler, E. (2024). Synthesis of hydroxyapatite from eggshells via wet chemical precipitation: A review. *RSC Advances*, *14*(30), 21439–21452. https://doi.org/10.1039/D4RA02198C

Kumar, G. S., & Girija, E. K. (2013). Flower-like hydroxyapatite nanostructure obtained from eggshell: A candidate for biomedical applications. *Ceramics International*, *39*(7), 8293–8299. https://doi.org/10.1016/j.ceramint.2013.03.099

Liu, J., Li, K., Wang, H., Zhu, M., & Yan, H. (2004). Rapid formation of hydroxyapatite nanostructures by microwave irradiation. *Chemical Physics Letters*, *396*(4-6), 429–432. https://doi.org/10.1016/j.cplett.2004.08.094

Madupalli, H., Pavan, B., & Tecklenburg, M. M. J. (2017). Carbonate substitution in the mineral component of bone: Discriminating the structural changes, simultaneously imposed by carbonate in A and B sites of apatite. *Journal of Solid State Chemistry*, *255*, 27–35. https://doi.org/10.1016/j.jssc.2017.07.025

Neel, E. A. A., Aljabo, A., Strange, A., Ibrahim, S., Coathup, M., Young, A. M., Bozec, L., & Mudera, V. (2016). Demineralization–remineralization dynamics in teeth and bone. *International Journal of Nanomedicine*, *11*, 4743–4763. https://doi.org/10.2147/IJN.S107624

Nikfallah, A., Mohammadi, A., Ahmadakhondi, M., & Ansari, M. (2023). Synthesis and physicochemical characterization of mesoporous hydroxyapatite and its application in toothpaste formulation. *Heliyon*, *9*(10), e20924. https://doi.org/https://doi.org/10.1016/j.heliyon.2023.e20924

Nofriyanti, & Lini, R. (2021). Formulasi dan uji sifat fisik pasta gigi gel dari ekstrak kering jahe merah (Zingiber Officinale Roscoe Var. Rubrum). *Jurnal Penelitian Farmasi Indonesia*, *10*(1), 6–11. https://doi.org/10.51887/jpfi.v10i1.994

Noviyanti, A.R, Fauzia, R. P., & Risdiana. et.al. (2020). A novel hydrothermal synthesis of nanohydroxyapatite from eggshell-calcium-oxide precursors. *Heliyon*, *6*(4). https://doi.org/10.1016/j.heliyon.2020.e03655.

Owuamanam, S., & Cree, D. (2020). Progress of bio-calcium carbonate waste eggshell and seashell fillers in polymer composites: a review. *Journal of Composites Science*, *4*(2), 70. https://doi.org/10.3390/jcs4020070

Perwiranegara, S. A., Bayuseno, A. P., & Ismail, R. (2021). Pengaruh Daya Microwave Terhadap Karakterisasi Hidroksiapatit Behbahan Cangkang Rajungan. *Jurnal Teknik Mesin S-1*, *9*(4), 1–6. Retrieved from https://ejournal3.undip.ac.id/index.php/jtm/article/view/36428

Rarung, A. M. M. L., Veronika, P., Yamlean, Y., Lifie, K., & Mansauda, R. (2022). Formulation And Antibacterial Activity Test of Cocoa Bean Extract Toothpaste (Theobroma Cacao L.) Against Streptococcus Mutans Formulasi Dan Uji Aktivitas Antibakteri Pasta Gigi Ekstrak Etanol Biji Kakao (Theobroma Cacao L.) Terhadap Bakteri Streptococcus. *Jurnal*

Pharmacon-Program Studi Farmasi, FMIPA, UNIVERSITAS SAM RATULANGI, *11*(4), 1793–1804. https://doi.org/10.35799/pha.11.2022.44318

Sabu, U., Logesh, G., Rashad, M., Joy, A., & Balasubramanian, M. (2019). Microwave assisted synthesis of biomorphic hydroxyapatite. *Ceramics International*, *45*(6), 6718–6722. https://doi.org/10.1016/j.ceramint.2018.12.161

Stanislavov, A. S., Sukhodub, L. F., Sukhodub, L. B., Kuznetsov, V. N., Bychkov, K. L., & Kravchenko, M. I. (2018). Structural features of hydroxyapatite and carbonated apatite formed under the influence of ultrasound and microwave radiation and their effect on the bioactivity of the nanomaterials. *Ultrasonics Sonochemistry*, *42*(October 2017), 84–96. https://doi.org/10.1016/j.ultsonch.2017.11.011

Tschoppe, P., Zandim, D. L., Martus, P., & Kielbassa, A. M. (2011). Enamel and dentine remineralization by nano-hydroxyapatite toothpastes. *Journal of Dentistry*, *39*(6), 430–437. https://doi.org/https://doi.org/10.1016/j.jdent.2011.03.008

Vinoth Kumar, K. C., Jani Subha, T., Ahila, K. G., Ravindran, B., Chang, S. W., Mahmoud, A. H., Mohammed, O. B., & Rathi, M. A. (2021). Spectral characterization of hydroxyapatite extracted from Black Sumatra and Fighting cock bone samples: A comparative analysis. *Saudi Journal of Biological Sciences*, *28*(1), 840–846. https://doi.org/https://doi.org/10.1016/j.sjbs.2020.11.020

Wang, Y., Tsuru, K., Ishikawa, K., Yokoi, T., & Kawashita, M. (2021). Fibronectin adsorption on carbonate-containing hydroxyapatite. *Ceramics International*, *47*(8), 11769–11776. https://doi.org/https://doi.org/10.1016/j.ceramint.2021.01.017

Waardhani, A. W., Noviyanti, A. R., Kusrini, E., Nugrahaningtyas, K. D., Prasetyo, A. B., Usman, A., ... & Juliandri, J. (2025). A study on sustainable eggshell-derived hydroxyapatite/CMC membranes: Enhancing flexibility and thermal stability for sustainable development goals (SDGs). *Indonesian Journal of Science and Technology*, *10*(2), 191-206. Retrieved from https://ijost.upi.edu/index.php/ijost/article/view/449

Zhou, H., & Lee, J. (2011). Nanoscale hydroxyapatite particles for bone tissue engineering. *Acta Biomaterialia*, *7*(7), 2769–2781. https://doi.org/https://doi.org/10.1016/j.actbio.2011.03.019